ISSN 1063-7834, Physics of the Solid State, 2020, Vol. 62, No. 9, pp. 1612–1618. © Pleiades Publishing, Ltd., 2020.
Russian Text © The Author(s), 2020, published in Fizika Tverdogo Tela, 2020, Vol. 62, No. 9, pp. 1447–1453.

SUPERCONDUCTIVITY

Spin–Orbit Coupling-Induced Effective Interactions in Superconducting Nanowires in the Strong Correlation Regime

A. O. Zlotnikov[a], *, S. V. Aksenov[a], and M. S. Shustin[a]

[a] *Kirensky Institute of Physics, Krasnoyarsk Scientific Center, Siberian Branch, Russian Academy of Sciences, Krasnoyarsk, 660036 Russia*

**e-mail: zlotn@iph.krasn.ru*

Received March 26, 2020; revised March 26, 2020; accepted April 2, 2020

Abstract—In the second order of the operator form of the perturbation theory, the effective interactions in a superconducting nanowire have been obtained at the strong electron correlations, when the spin–orbit coupling parameter is comparable with the hopping integral. Using the exact diagonalization technique, in short nanowires with the open boundary conditions at the strong Coulomb repulsion, the excitations corresponding to the Majorana edge states with the energy below the value of a bulk superconducting gap have been demonstrated.

Keywords: superconducting nanowire, spin–orbit coupling, Majorana modes, strong electron correlations
DOI: 10.1134/S1063783420090371

1. INTRODUCTION

Recently, there has been a great interest in the InAs and InSb semiconductor nanowires brought into contact with a superconductor, in which a quantized differential conductivity peak is experimentally observed at zero bias voltage in an applied magnetic field [1]. This feature of the conductance is often explained by the transition of a system to the topological superconductivity phase upon continuous variation in one of the parameters, e.g., a magnetic field. When this scenario is implemented, then, at the transition point, in a critical field, the gap in the bulk spectrum vanishes and, with a further increase in the control parameter and moving away from the transition point, the spectrum becomes gapped again. In the topologically nontrivial phase, the edge state arises that has zero energy and includes a pair of Majorana modes localized at the opposite ends of a wire [2–4]. It is this spatial nonlocality that determines, to a great extent, the practical interest in the Majorana states, since it makes them resistant against local perturbations, which tend to disrupt the phase of the wave function of a quasiparticle, which is fundamentally important for quantum calculations [5]. It should be noted that the appearance of a quantized conductance peak can also be caused by the trivial Andreev states or a general increase in the density of states at zero energy due to antilocalization [6–8]. As a result, this ambiguity in the interpretation of tunnel spectroscopy experiments with hybrid nanowires leads to the necessity of taking into account the impact of various practical factors [9, 10] and considering more complex systems in which the difference in transport through the Majorana and Andreev states becomes noticeable [11].

It is important that, in most cases, when studying the Majorana modes in 1D and quasi-1D wires, the effect of electron–electron interactions is ignored. However, recently, it has been shown by the analysis of the I–V characteristics of a structure consisting of parallel InAs nanowires that, in such a structure, strong correlations and the Luttinger liquid mode with the spin–orbit coupling are implemented [12]. Therefore, it is relevant to study the effect of the strong Coulomb repulsion between electrons on the formation of Majorana modes in the systems under study.

To take into account the electron–electron interaction in these systems, the generalized 1D Hubbard model in the presence of the Rashba spin–orbit coupling and the external field is often used. The mean-field approaches [13] and numerical methods, including the density matrix renormalization group (DMRG), are used [14]. It was shown that, the allowance for the weak interaction leads to the fact that the topologically nontrivial phase and Majorana modes form in weaker magnetic fields than in the non-interacting case. These results are confirmed also in the description based on boson fields and renormalization group equations. The investigations of the opposite strong interaction regime leads to the destruction of the superconducting state and the occurrence of a free fermion gas with a gapless spectrum and the absence of edge states [13–15].

It is worth noting that, despite the presence of a magnetic field, the proposed 1D model of a supercon-

ducting nanowire belongs to the BDI, rather than D, symmetry class [16]. However, the differences between the two classes manifest themselves only when the superconducting spin–singlet pairings between electrons located on neighboring and more distant chain sites are taken into account. Such pairings related to the extended *s*-wave symmetry can be formed by considering the proximity effect with a bulk superconductor characterized by the existence of the nonlocal pairing interaction or by taking into account the inhomogeneity of the interface in a hybrid structure [17]. In view of this, it is interesting to study the effect of strong electron correlations, when the Coulomb repulsion parameter is much larger than the rest model parameters, on the superconducting state and edge modes in a nanowire, if superconductivity is induced not only by on-site pairings, but also by pairings between the nearest neighbors. Previously, we studied this structure using the DMRG approach. In particular, the possibility of inducing the double Majorana modes due to the Coulomb interaction was demonstrated [18].

In the framework of the operator form of the perturbation theory for superconducting nanowires in the strong correlation regime, we construct the t–J^*–J^*_α model operating in the truncated Hilbert space, which does not contain the states with two electrons on a site and takes into account the transitions between the Hubbard subbands by inducing the effective interactions, including three-center ones. In the model, the effective interactions are caused not only by electron hoppings, but also by the spin–orbit coupling, since the corresponding parameters in the investigated systems are comparable. In addition, corrections from the induced superconducting pairings were obtained. A series of transitions with a change in the parity of the ground state upon variation in the chemical potential were demonstrated by the exact diagonalization method. At the transition points, the zero-energy excitations were implemented. The results obtained show the possibility of the formation of Majorana edge states in the strong electron correlation regime for short (10–14 sites) nanowires. Such states are caused by the induced superconducting pairings between electrons on the nearest sites, since the on-site pairings are suppressed by the Coulomb interaction.

2. DERIVATION OF THE EFFECTIVE HAMILTONIAN OF THE t–J^*–J^*_α MODEL

We write the Hamiltonian of the 1D Hubbard model in the atomic representation, taking into account the Zeeman splitting, the Rashba spin–orbit coupling, and the superconducting potential induced by the proximity effect, which is a minimum model for describing the investigated systems

$$H = H_0 + H_1 + H_2 + H'. \tag{1}$$

The single-site Hamiltonian is expressed as

$$H_0 = \sum_{f\sigma} \xi_\sigma X_f^{\sigma\sigma} + \sum_f (2\xi + U) X_f^{22}, \tag{2}$$

where $\xi_\sigma = \xi - \eta_\sigma h$; $\xi = \varepsilon_0 - \mu$; ε_0 is the bare energy of electrons, μ is the chemical potential; h is the Zeeman splitting parameter; $\eta_\sigma = \pm 1$ at $\sigma = \uparrow, \downarrow$, respectively; and U is the on-site Hubbard repulsion parameter. The Hubbard operators are defined in the standard form $X_f^{nm} = |f,n\rangle\langle f,m|$, where $|f,n\rangle$ are the basis electronic states on site f: $n = 0$ is the state without electrons, $n = \sigma$ is the state with one electron with the spin moment projection σ, and $n = 2$ is the two-electron state. The action of the Hubbard operators on the basis of states is determined in the form $X_f^{nm}|f',p\rangle = \delta_{ff'}\delta_{mp}|f,n\rangle$, where δ_{ij} are the Kronecker symbols. The relation between the Hubbard operators and the Fermi electron operators $a_{f\sigma}$ and $a^\dagger_{f\sigma}$ has the form $X_f^{\sigma\sigma} = n_{f\sigma}(1 - n_{f\bar\sigma})$, $X_f^{22} = n_{f\uparrow}n_{f\downarrow}$, $X_f^{0\sigma} = a_{f\sigma}(1 - n_{f\bar\sigma})$, and $X_f^{\bar\sigma 2} = \eta_\sigma a_{f\sigma} n_{f\bar\sigma}$, where $n_{f\sigma} = a^\dagger_{f\sigma}a_{f\sigma}$. The expressions for the rest Hubbard operators can be easily determined from the presented expressions.

As is known, with an increase in the on-site Coulomb repulsion, at a certain critical value, the initial electron band is divided into two subbands with a gap between them [19]. With a further increase in the interaction parameter, the gap increases a Mott–Hubbard dielectric state is formed at half-filling. The arising subbands are called Hubbard. In the atomic representation, the Hubbard subbands can be explicitly distinguished for any parameters, even in the absence of a gap between them. This is due to the fact that the lower subband is defined for the states related to the homeopolar sector of the Hilbert space, which does not contain the states $|f,2\rangle$ with two electrons on a site. For the upper subband, such states are taken into account, but the states $|f,0\rangle$ without electrons are excluded. The terms H_1 and H_2 introduced in Eq. (1) describe the processes in the lower and upper Hubbard subbands, respectively:

$$\begin{aligned} H_1 = &-\frac{t}{2}\sum_{f\sigma}(X_f^{\sigma 0}X_{f+1}^{0\sigma} + X_{f+1}^{\sigma 0}X_f^{0\sigma}) \\ &-\frac{\alpha}{2}\sum_{f\sigma}\eta_\sigma(X_f^{\sigma 0}X_{f+1}^{0\bar\sigma} + X_{f+1}^{\bar\sigma 0}X_f^{0\sigma}) \\ &+\Delta_1\sum_f(X_f^{0\uparrow}X_{f+1}^{0\downarrow} + X_{f+1}^{0\uparrow}X_f^{0\downarrow}) \\ &+\Delta_1^*\sum_f(X_{f+1}^{\downarrow 0}X_f^{\uparrow 0} + X_f^{\downarrow 0}X_{f+1}^{\uparrow 0}), \\ H_2 = &-\frac{t}{2}\sum_{f\sigma}(X_f^{2\bar\sigma}X_{f+1}^{\bar\sigma 2} + X_{f+1}^{2\bar\sigma}X_f^{\bar\sigma 2}) \end{aligned} \tag{3}$$

$$-\frac{\alpha}{2}\sum_{f\sigma}\eta_{\bar{\sigma}}(X_f^{2\bar{\sigma}}X_{f+1}^{\sigma 2}+X_{f+1}^{2\sigma}X_f^{\bar{\sigma}2}) - \Delta_1\sum_f(X_f^{\downarrow 2}X_{f+1}^{\uparrow 2}+X_{f+1}^{\downarrow 2}X_f^{\uparrow 2}) - \Delta_1^*\sum_f(X_{f+1}^{2\uparrow}X_f^{2\downarrow}+X_f^{2\uparrow}X_{f+1}^{2\downarrow}). \quad (4)$$

The terms with the parameters t and α ($t, \alpha > 0$) determine hoppings and the Rashba spin–orbit coupling, respectively, which involve electrons on neighboring sites and the terms with the parameter Δ_1 describe the induced superconducting pairings of electrons on the nearest sites in the singlet state.

The transition between the Hubbard subbands is determined by H'

$$H' = -\frac{t}{2}\sum_{f\sigma}\eta_\sigma(X_f^{\sigma 0}X_{f+1}^{\bar{\sigma}2}+X_f^{2\bar{\sigma}}X_{f+1}^{0\sigma} + X_{f+1}^{2\bar{\sigma}}X_f^{0\sigma}+X_{f+1}^{\sigma 0}X_f^{\bar{\sigma}2}) - \frac{\alpha}{2}\sum_{f\sigma}(-X_f^{\sigma 0}X_{f+1}^{\sigma 2} + X_f^{2\sigma}X_{f+1}^{0\sigma} - X_{f+1}^{2\sigma}X_f^{0\sigma}+X_{f+1}^{\sigma 0}X_f^{\sigma 2}) + \left\{-\Delta\sum_f X_f^{02} + \Delta_1\sum_f(-X_f^{0\uparrow}X_{f+1}^{\uparrow 2} - X_{f+1}^{0\uparrow}X_f^{\uparrow 2} + X_f^{\downarrow 2}X_{f+1}^{0\downarrow}+X_{f+1}^{\downarrow 2}X_f^{0\downarrow})\right\} + \{\text{h.c.}\}, \quad (5)$$

where h.c. denotes the Hermitian conjugation of the previous expression. Here, the terms with the parameter Δ characterize the superconducting potential induced on a site, which is usually taken into account in the description of superconducting nanowires [13, 14]. It can be seen from formula (5) that, with an increase in the Coulomb repulsion parameter U, such pairings should rapidly collapse upon broadening of the gap between the Hubbard subbands. The interaction will also suppress the pairings between electrons on the neighboring sites with the parameter Δ_1 included in the term H' and described the transitions between the Hubbard subbands. However, since some nonlocal pairings involve the states only in the lower Hubbard subband (see Eq. (3)), the superconductivity induced by such processes will be retained at arbitrarily large values of the Hubbard repulsion if the inter-site Coulomb interaction is small as compared with Δ_1.

We use the operator form of the perturbation theory [20] for the regime $U \gg t, \alpha, \Delta, \Delta_1$. In this regime, the desired effective Hamiltonian is determined on the Hilbert subspace that does not contain the states with two electrons on a site. Then, the projection operator has the form

$$P = \prod_f(X_f^{00}+X_f^{\uparrow\uparrow}+X_f^{\downarrow\downarrow}). \quad (6)$$

The contributions of the transitions between the Hubbard subbands are taken into account due to the occurrence of additional interactions with the smallness parameters t/U, α/U, Δ/U, and Δ_1/U in different degrees. Using these parameters, the effective Hamiltonian is determined with the quadratic accuracy as

$$H_{\text{eff}} = PH_0P + H_1 - \frac{1}{2}(PH'(H_0 - KH_0K)^{-1}H'P + \text{h.c.}), \quad (7)$$

where K is the Hermitian conjugation operator.

After the standard calculations, the effective Hamiltonian is

$$H_{t-J^*-J_\alpha^*} = \sum_{f\sigma}\xi_\sigma X_f^{\sigma\sigma} - \frac{\Delta^2+2\Delta_1^2}{2\xi+U}\sum_f X_f^{00} + H_1 + H_{\text{int}} + H_3. \quad (8)$$

Here, the second term describes the renormalizations to the bare energy of the system due to the superconducting pairings. Note that the term H_1 (Eq. (3)) enters the effective Hamiltonian in the unchanged form. The term H_{int} resulting from the calculations describes two-center interactions in the lower Hubbard subband and has the form

$$H_{\text{int}} = \frac{2(t/2)^2}{U}\sum_{f\sigma}(X_f^{\sigma\bar{\sigma}}X_{f+1}^{\bar{\sigma}\sigma} - X_f^{\sigma\sigma}X_{f+1}^{\bar{\sigma}\bar{\sigma}}) - \frac{t\alpha}{2}\sum_{f\sigma}\frac{U+\eta_\sigma h}{U(U+2\eta_\sigma h)} \times \eta_\sigma\{(X_f^{\sigma\bar{\sigma}}+X_f^{\bar{\sigma}\sigma})X_{f+1}^{\sigma\sigma} - X_f^{\sigma\sigma}(X_{f+1}^{\sigma\bar{\sigma}}+X_{f+1}^{\bar{\sigma}\sigma})\} - 2(\alpha/2)^2\sum_{f\sigma}\frac{1}{U-2\eta_\sigma h} \times\left\{\frac{1}{2}(X_f^{\sigma\bar{\sigma}}X_{f+1}^{\sigma\bar{\sigma}}+X_f^{\bar{\sigma}\sigma}X_{f+1}^{\bar{\sigma}\sigma}) + X_f^{\bar{\sigma}\bar{\sigma}}X_{f+1}^{\bar{\sigma}\bar{\sigma}}\right\} + \frac{t\Delta}{2}\left(\frac{1}{2\xi+U}+\frac{1}{U}\right)\sum_f(X_f^{0\uparrow}X_{f+1}^{0\downarrow} - X_f^{0\downarrow}X_{f+1}^{0\uparrow} + \text{h.c.}) - \frac{\alpha\Delta}{2}\sum_{f\sigma}\left(\frac{1}{2\xi+U}+\frac{1}{U+2\eta_\sigma h}\right)(X_f^{0\sigma}X_{f+1}^{0\sigma}+\text{h.c.}) + \frac{2\Delta\Delta_1}{2\xi+U}\sum_{f\sigma}(X_f^{\sigma 0}X_{f+1}^{0\sigma}+\text{h.c.}) + \frac{2\Delta_1^2}{2\xi+U}\sum_f X_f^{00}X_{f+1}^{00}. \quad (9)$$

The terms in H_{int} that are proportional to t^2/U describe the well-known kinetic antiferromagnetic exchange interaction [19, 21]. The terms with $\alpha^2/(U \pm 2h)$ determine the interaction between electrons on neighboring sites with the same spin moment projection, which results in the change of both electrons projections for the opposite ones. At the interactions with the param-

eter $\sim t\alpha/U$, the spin moment projection changes only for one electron from the pair on neighboring sites. In terms of the magnetic characteristics, the interaction induced by the spin–orbit coupling can compete with the antiferromagnetic exchange interaction and facilitate the formation of a noncollinear short-range magnetic order in 1D systems. The term with the parameter $\sim t\Delta/U$ describes spin-singlet superconducting pairings between the nearest sites, which corresponds to the symmetry of the superconducting order parameter in initial Hamiltonian (1). The existence of effective spin-triplet pairings with allowance for the spin–orbit coupling in an external magnetic field is an important factor in the implementation of the Majorana bound states in 1D systems [2]. In the strongly correlated regime, the triplet pairings with an amplitude of $\sim\alpha\Delta/U$ explicitly arise due to the spin–orbit coupling. This determines the important role played by the spin–orbit coupling in the implementation of the Majorana states in superconducting nanowires. However, since the amplitude of such pairings at the strong correlations is small, the existence of edge modes is caused mainly by the spin-singlet superconducting pairings inside the lower subband with the parameter Δ_1 (see Eq. (3)), which induce the effective triplet superconductivity in the presence of the spin–orbit coupling and Zeeman splitting.

The three-center terms are determined as

$$\begin{aligned}
H_3 = &-\frac{(t/2)^2}{U}\sum_{f\sigma}(X^{\sigma 0}_{f-1}X^{\bar\sigma\bar\sigma}_{f}X^{0\sigma}_{f+1}\\
&- X^{\bar\sigma 0}_{f-1}X^{\sigma\bar\sigma}_{f}X^{0\sigma}_{f+1} + \text{h.c.})\\
&+ (t/2)(\alpha/2)\sum_{f\sigma}\frac{\eta_\sigma}{2(U-2\eta_\sigma h)}\{X^{\bar\sigma 0}_{f-1}(X^{\bar\sigma\bar\sigma}_{f}\\
&- X^{\bar\sigma\bar\sigma}_{f})X^{0\bar\sigma}_{f+1} - X^{\sigma 0}_{f-1}X^{\bar\sigma\bar\sigma}_{f}X^{0\bar\sigma}_{f+1} + X^{\bar\sigma 0}_{f-1}X^{\bar\sigma\bar\sigma}_{f}X^{0\sigma}_{f+1} + \text{h.c.}\}\\
&+ \frac{(t/2)(\alpha/2)}{2U}\sum_{f\sigma}\eta_\sigma\{X^{\sigma 0}_{f-1}(X^{\sigma\bar\sigma}_{f} - X^{\bar\sigma\sigma}_{f})X^{0\sigma}_{f+1}\\
&- X^{\sigma 0}_{f-1}(X^{\sigma\sigma}_{f} + X^{\bar\sigma\bar\sigma}_{f})X^{0\bar\sigma}_{f+1} + \text{h.c.}\}\\
&+ \sum_{f\sigma}\frac{(\alpha/2)^2}{U-2\eta_\sigma h}(X^{\bar\sigma 0}_{f-1}X^{\bar\sigma\bar\sigma}_{f}X^{0\bar\sigma}_{f+1} + \text{h.c.})\\
&+ \frac{(\alpha/2)^2 U}{U^2-4h^2}\sum_{f\sigma}(X^{\sigma 0}_{f-1}X^{\sigma\bar\sigma}_{f}X^{0\bar\sigma}_{f+1} + \text{h.c.})\\
&+ \frac{\Delta_1^2}{2\xi+U}\sum_{f\sigma}(X^{\sigma 0}_{f-1}X^{\sigma\sigma}_{f}X^{0\sigma}_{f+1} + X^{\sigma 0}_{f-1}X^{\bar\sigma\sigma}_{f}X^{0\bar\sigma}_{f+1} + \text{h.c.}).
\end{aligned} \tag{10}$$

The important role of the three-center interactions $\sim t^2/U$ in the description of the superconducting phase in the 2D t–J* model was demonstrated in [22]. In contrast to such terms, the terms $\sim t\alpha/U$ describe electron hoppings to the next-to-nearest site with the conservation (change) of the spin moment projection, when the electron spin moment projection at the nearest site becomes opposite (does not change). The terms $\sim\alpha^2/U$ are similar to the three-center interactions induced only by hopping, except for the fact that they make the contribution when electrons on two neighboring sites have the same spin projection onto the quantization axis.

The terms proportional to Δ enter the effective Hamiltonian only with the factor $\sim\Delta/U$ and their values are small. Thus, it has been clearly demonstrated that the on-site pairings are suppressed by the Coulomb repulsion. The superconductivity is determined, in fact, by the spin-singlet pairings between the nearest sites belonging to the extended s-wave symmetry with the parameter Δ_1. The corresponding terms are included in H_1.

The effective Hamiltonian is applicable in the magnetic fields leading to the Zeeman splitting with $h > 0$ at which $U - 2h \gg t$, α, Δ, Δ_1. It can be seen that the smallness parameter $1/(2\xi + U)$ increases with the electron density. However, the effective Hamiltonian is only applicable to the lower Hubbard subband, the top of which is usually reached in the μ range from approximately $0.5t$ to t; therefore, the smallness of the parameter is valid at $2\xi + U \gg 1$.

3. EXACT DIAGONALIZATION OF SHORT CHAINS AT THE STRONG CORRELATIONS

The transition to effective model (8) significantly simplifies the numerical calculations at the strong correlations due to the reduction of the Hilbert space size from 4^N to 3^N (N is the number of sites in a chain). However, the exact diagonalization method for the obtained Hamiltonian is still resource-consuming; therefore, here we consider the case of short chains. The exact diagonalization allows one to determine the particle eigenfunctions of the Hamiltonian, characterizing them by the fermionic parity, and the corresponding energies of the even (E_j^{ev}) and odd (E_j^{od}) sectors of the Hilbert space. For the further consideration, let us determine that the many-body state has positive or negative fermionic parity if its partial contributions contain only the states with an even or odd number of fermions, respectively.

For comparison, Figs. 1 and 2 show the energies $2N$ of the smallest excitations for initial (1) (asterisks) and effective (8) (circles) models in a chain with ten sites for the Coulomb repulsion parameter U equal to $10t$ and $100t$, respectively. The remaining parameters do not change: $\alpha = 0.8t$, $h = 0.8t$, $\mu = -t$, $\Delta = 0.5t$, and $\Delta_1 = 0.25t$. It can be seen that the first three excitations for the two models are in good agreement even at $U = 10t$. At $U = 100t$, the agreement becomes better for the next three excitations. It should be noted that the numerically exact agreement is obtained at $U \to \infty$.

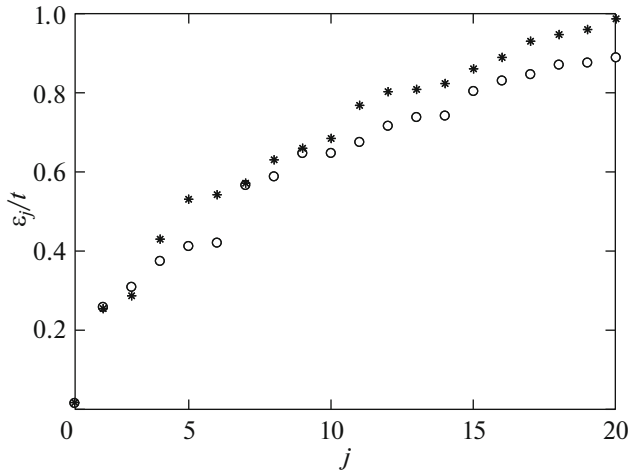

Fig. 1. Energies $2N$ (N is the number of sites) of the least excitations describing the transitions between the ground many-body state of the system and corresponding induced states in a chain with $N = 10$ sites for initial Hubbard model (1) (asterisks) and effective t–J^*–J^*_α model (8) (circles). The parameters are $U = 10t$, $\alpha = 0.8t$, $h = 0.8t$, $\Delta = 0.5t$, and $\Delta_1 = 0.25t$ in units of the hopping integral.

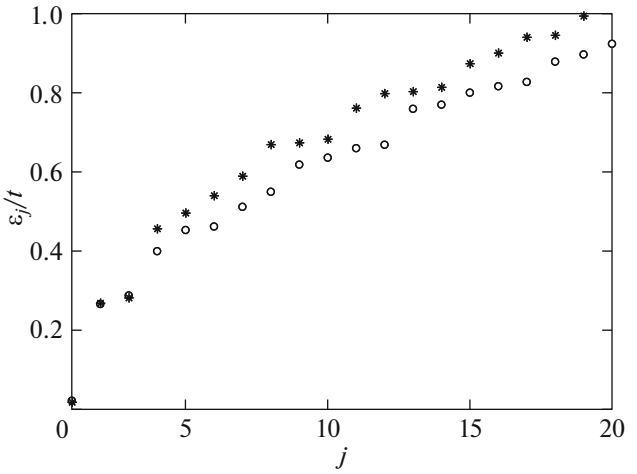

Fig. 2. Energies of the least excitations in a chain with $N = 10$ sites for the initial Hubbard model (asterisk) and the effective t–J^*–J^*_α model (circles) at $U = 100t$. The rest parameters are as in Fig. 1.

Below, the first two excitation energies are analyzed.

The conditions for the implementation of the Majorana edge states in short chains in the regime of strong correlations are sought for by comparing the single-particle excitation spectrum for chains with the open and periodic boundary conditions (PBC). It is well-known that a gap in the single-particle excitation spectrum is implemented for a chain with the PBC in both topologically trivial and nontrivial phases and the spectrum becomes gapless at the boundaries between phases. In the topologically nontrivial phase, the ground state of a chain with the PBC with an even number of sites without interaction has the negative fermionic parity [23], in contrast to the positive parity of the ground state in the trivial phase. The latter turned out to be true also in the investigations of the system in the regime of strong electron correlations. When passing to the chains with the open boundary conditions, the single-particle excitations can be implemented, the energy of which lies in the gap in the bulk spectrum of the system. According to a classification of the edge states, this condition is a criterion for the fact that the excitation under study is an edge one [24]. The energy oscillation of such excitations is related to the interference of wave functions of the Majorana modes, which tend to localization at the opposite ends of the chain.

Thus, the presence of the Majorana edge states in short chains can be judged by the following criteria: (i) at least one energy of the single-particle excitations in an open chain lies inside the spectrum gap with the PBC; (ii) the minimum excitation energy oscillates around zero in a certain region of parameters, which is indicative of the change in the parity of the ground state when the energy exactly vanishes; and (iii) in this range of parameters, the ground state of the chain with the PBC has the negative fermionic parity. It should be noted that the edge states determined in this way for a short chain are not true Majorana states, since their excitation energy can be significantly different from zero and the wave functions of different modes are not explicitly localized at one of the chain edges. However, it is assumed that, with an increase in the number of sites in a chain, these states become Majorana due to the size effects. The introduced criteria allowed us to study the conditions for the implementation of the edge states in superconducting nanowires with the interaction by examining only very short (10–20 sites) chains using the exact diagonalization method.

Figure 3 presents the evidences of meeting the above criteria in the discussed model for short chains. The dark solid line corresponds to the difference between the lowest energies of many-body states with the negative and positive fermionic parity $\Delta E_1 = E_1^{\text{od}} - E_1^{\text{ev}}$ for a chain of twelve sites. The bright solid curve corresponds to the energy of the second single-particle excitation relative to the ground state. Solid (dashed) lines correspond to a system with the open (periodic) boundary conditions. It can be seen that the ground state of the system with the PBC has the positive fermion parity at small and large μ values. Between these μ ranges, there is a region of implementation of a topologically nontrivial phase with $\Delta E_1 < 0$ in the system. For an open chain, the ΔE_1 value oscillates and the zero-energy excitations are implemented. The number of points with the change in the fermionic parity depends on the number of sites in the chain. In

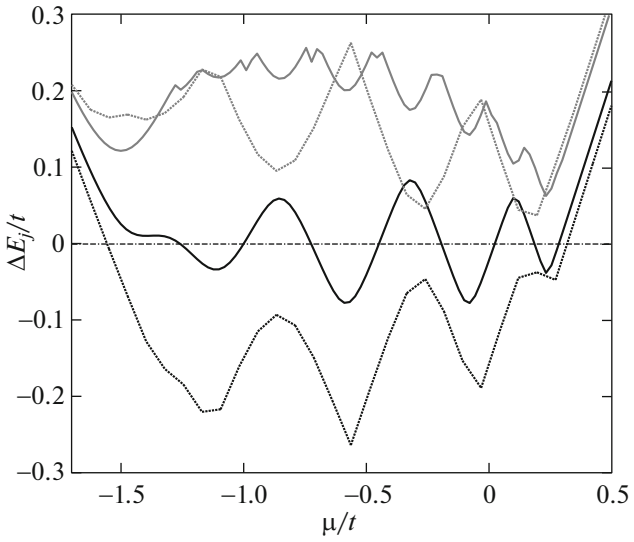

Fig. 3. Energy difference $\Delta E_1 = E_1^{od} - E_1^{ev}$ (dark lines) showing the change in the parity of the ground state and ΔE_2 (light lines) determined as $E_2^{od} - E_1^{ev}$ at $\Delta E_1 > 0$ or $E_2^{ev} - E_1^{od}$ at $\Delta E_1 < 0$ as a function of the chemical potential for an open chain with 12 sites (solid lines) and a chain folded into a ring (dashed lines). The parameters are as in Fig. 1.

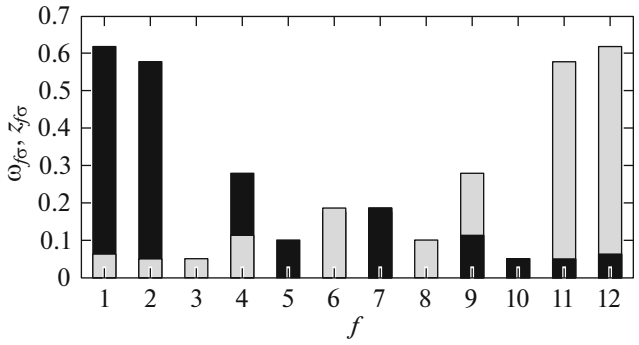

Fig. 4. Spatial dependence of the coefficients $\omega_{f\sigma}$ and $z_{f\sigma}$ characterizing the matrix elements of Majorana operators at the transition from the ground to first excited state at $\mu = -1.256t$ (see Fig. 3) in an open nanowire with 12 sites.

particular, when we consider six sites, the fermionic parity for an open chain changes only twice in the region corresponding to the nontrivial phase of the PBC system.

The spatial structure of single-electron excitations can be analyzed using the coefficients

$$w_{f\sigma} = \left\langle \Psi_1^{od(ev)} \middle| (X_f^{0\sigma} + X_f^{\sigma 0}) \middle| \Psi_1^{ev(od)} \right\rangle, \quad (11)$$

$$z_{f\sigma} = i \left\langle \Psi_1^{od(ev)} \middle| (X_f^{0\sigma} - X_f^{\sigma 0}) \middle| \Psi_1^{ev(od)} \right\rangle, \quad (12)$$

where $\left| \Psi_1^{ev(od)} \right\rangle$ is the eigenvector of the ground state of a wire in the even (odd) Hilbert space sector. Their dependence on the coordinate for the zero-energy excitation at $\mu = -1.256t$ is presented in Fig. 4. One can see a trend to the implementation of the Majorana edge states, which will become more pronounced with increasing chain length. The latter result demonstrates the stability of such modes with respect to the strong electron correlations.

4. CONCLUSIONS

In this study, we investigated the stability of the single-particle Majorana excitations against the strong electron correlations for a short nanowire placed in an external magnetic field with the strong Rashba spin–orbit coupling and induced singlet superconductivity of the extended *s*-wave symmetry. The system was described using the one-dimensional Hubbard model, which takes into account the terms corresponding to the spin–orbit coupling and singlet superconducting pairings induced by the proximity effect. Using this model, we obtained the effective interactions in the second order of the perturbation theory for which the operator structure is defined on the homeopolar sector of the Hilbert space. In addition to the well-known terms describing the kinetic exchange interaction of electrons, the contribution to the effective interactions in the investigated system are made by the terms describing the trend to the noncollinear magnetic ordering, singlet and triplet superconducting pairings, and three-center interactions. In the derived model, the elementary excitation spectrum was examined by the exact diagonalization method and the possibility of implementation of a topologically nontrivial phase was analyzed. It is important that the exact numerical results were obtained at the strong Coulomb repulsion. It was shown that even in the regime of strong electronic correlations, the single-particle Majorana excitations can occur in the system; the energy of such excitations is below the spectrum gap under the periodic boundary conditions and its dependences on the chemical potential and magnetic field oscillate around zero. Such a behavior is observed exactly for the region in which the many-body ground state of the system with the periodic boundary conditions has the negative fermion parity.

FUNDING

This study was supported by the Russian Foundation for Basic Research, projects nos. 19-02-00348 and 20-3270059, the Government of the Krasnoyarsk Territory and the Krasnoyarsk Territorial Foundation for Support of Scientific and R&D Activity, projects nos. 19-42-240011 and 18-42-240014 “Single-Orbit Effective Model of an Ensemble of Spin-Polaron Quasiparticles in the Problem of Describing the Intermediate State and Pseudogap Behavior of Cuprate

Superconductors," and the Presidium of the Russian Academy of Sciences, program I.12 "Fundamental Problems of High-Temperature Superconductivity." S.V.A. thanks the Council for Grants of the President of the Russian Federation for Governmental Support of Young Russian Scientists, project no. MK-1641.2020.2.

CONFLICT OF INTEREST

The authors declare that they have no conflicts of interest.

REFERENCES

1. H. Zhang, C.-X. Liu, S. Gazibegovic, D. Xu, J. A. Logan, G. Wang, N. van Loo, J. D. Bommer, M. W. de Moor, D. Car, R. L. M. O. het Veld, P. J. van Veldhoven, S. Koelling, M. A. Verheijen, M. Pendharkar, et al., Nature (London, U.K.) **556**, 74 (2018).
2. R. M. Lutchyn, J. D. Sau, and S. Das Sarma, Phys. Rev. Lett. **105**, 077001 (2010).
3. Y. Oreg, G. Refael, and F. von Oppen, Phys. Rev. Lett. **105**, 177002 (2010).
4. V. V. Val'kov, V. A. Mitskan, and M. S. Shustin, J. Exp. Theor. Phys. **129**, 426 (2019).
5. A. Y. Kitaev, Ann. Phys. **303**, 2 (2003).
6. D. I. Pikulin, J. P. Dahlhaus, M. Wimmer, H. Schomerus, and C. W. J. Beenakker, New J. Phys. **14**, 125011 (2012).
7. J. Chen, B. D. Woods, P. Yu, M. Hocevar, D. Car, S. R. Plissard, E. P. A. M. Bakkers, T. D. Stanescu, and S. M. Frolov, Phys. Rev. Lett. **123**, 107703 (2019).
8. H. Pan, W. S. Cole, J. D. Sau, and S. Das Sarma, Phys. Rev. B **101**, 024506 (2020).
9. C.-X. Liu, J. D. Sau, T. D. Stanescu, and S. D. Sarma, Phys. Rev. B **96**, 075161 (2017).
10. C. Moore, T. Stanescu, and S. Tewari, Phys. Rev. B **97**, 165302 (2018).
11. V. V. Val'kov, M. Y. Kagan, and S. V. Aksenov, J. Phys.: Condens. Matter **31**, 225301 (2019).
12. Y. Sato, S. Matsuo, C.-H. Hsu, P. Stano, K. Ueda, Y. Takeshige, H. Kamata, J. S. Lee, B. Shojaei, K. Wickramasinghe, J. Shabani, Ch. Palmstrom, Y. Tokura, D. Loss, and S. Tarucha, Phys. Rev. B **99**, 155304 (2019).
13. R. M. Lutchyn and M. P. A. Fisher, Phys. Rev. B **84**, 214528 (2011).
14. E. Stoudenmire, J. Alicea, O. Starykh, and M. Fisher, Phys. Rev. B **84**, 014503 (2011).
15. S. Gangadharaiah, B. Braunecker, P. Simon, and D. Loss, Phys. Rev. Lett. **107**, 036801 (2011).
16. C. Wong and K. Law, Phys. Rev. B **86**, 184516 (2012).
17. A. M. Martin and J. F. Annett, Phys. Rev. B **57**, 8709 (1998).
18. S. V. Aksenov, A. O. Zlotnikov, and M. S. Shustin, Phys. Rev. B **101**, 125431 (2020).
19. Yu. A. Izyumov, Phys. Usp. **40**, 445 (1997).
20. N. N. Bogolyubov, *Collection of Scientific Works* (Nauka, Moscow, 2006), Vol. 6 [in Russian].
21. K. A. Chao, J. Spalek, and A. M. Oles, J. Phys. C **10**, L271 (1977).
22. V. V. Val'kov, T. A. Val'kova, D. M. Dzebisashvili, and S. G. Ovchinnikov, JETP Lett. **75**, 378 (2002).
23. A. Yu. Kitaev, Phys. Usp. Suppl. **44**, 131 (2001).
24. A. D. Fedoseev, J. Exp. Theor. Phys. **128**, 125 (2019).

Translated by E. Bondareva